

26th IAEA Fusion Energy Conference, Kyoto Japan, 17–22 October 2016

# Coupling of Neutral-beam-driven Compressional Alfvén Eigenmodes to Kinetic Alfvén Waves in NSTX and Energy Channeling

E. V. Belova<sup>1</sup>, N. N. Gorelenkov<sup>1</sup>, N. A. Crocker<sup>2</sup>, J. B. Lestz<sup>1</sup>, E. D. Fredrickson<sup>1</sup>, K. Tritz<sup>3</sup>

1) Princeton Plasma Physics Laboratory, Princeton NJ, USA

2) University of California, Los Angeles, California 90095, USA

3) Johns Hopkins University, Baltimore MD, USA

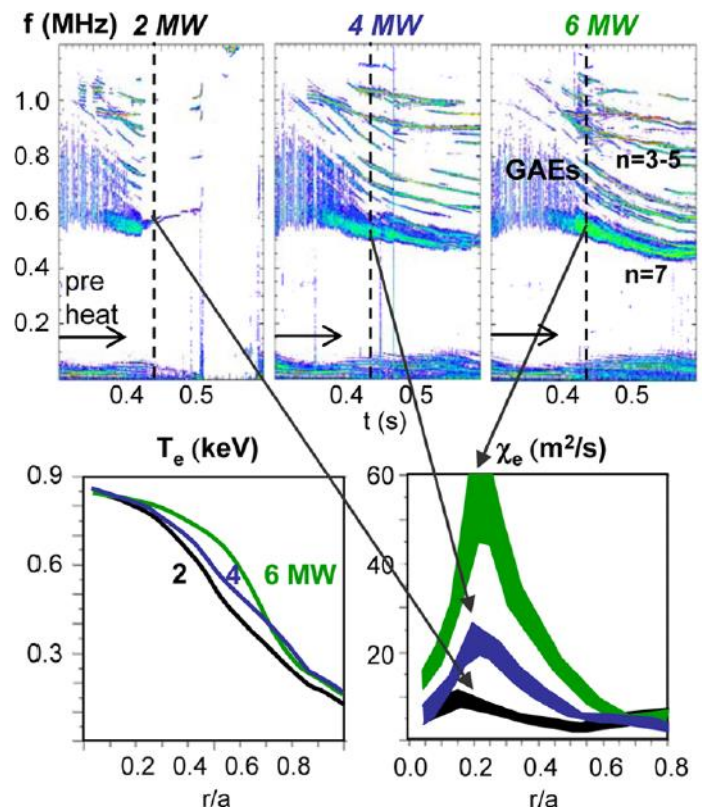
## Abstract

---

An energy channelling mechanism is proposed to explain flattening of the electron temperature profiles at high beam power in beam-heated National Spherical Torus Experiment (NSTX). High-frequency Alfvén eigenmodes are frequently observed in beam-heated NSTX plasmas, and have been linked to enhanced thermal electron transport and flattening of the electron temperature profiles. Results of 3D nonlinear self-consistent simulations of neutral-beam-driven compressional Alfvén eigenmodes (CAEs) in NSTX are presented that demonstrate strong coupling of CAE to kinetic Alfvén wave at the Alfvén resonance location. It is shown that CAE can channel significant fraction of the beam energy to the location of the resonant mode conversion at the edge of the beam density profile, modifying the energy deposition profile.

## Correlation between strong GAE/CAE activity and flattening of the electron temperature profile has been observed in NSTX [Stutman, PRL 2009]

- Intense GAE/CAE activity (0.5-1.1MHz).
- Flattening of  $T_e$  profile with
  - increased beam power;
  - beam energy scanned between 60 and 90 keV [Stutman, PRL 2009].
- Was attributed to enhanced electron transport.
  - Test particle simulations predict thermal electron transport due to orbit stochasticity in the presence of multiple GAEs [Gorelenkov, NF 2010].
- Different mechanism is considered here: Energy channeling due to coupling to KAW.
- Anomalously low  $T_e$  potentially can have significant implications for future fusion devices, especially low aspect ratio tokamaks.



Correlation between GAE activity,  $T_e$  flattening, and central electron heat diffusivity  $\chi_e$  in NSTX H modes with 2, 4, and 6MW neutral beam.

# HYM – Parallel Hybrid/MHD Code

---

**HYM code developed at PPPL and used to investigate kinetic effects on MHD modes in toroidal geometry (FRCs and NSTX)**

- 3-D nonlinear, parallel.
- Several different physical models:
  - Resistive MHD & Hall-MHD.
  - Hybrid (fluid electrons, particle ions).
  - MHD/particle (one-fluid thermal plasma, + energetic particle ions).
- Full-orbit kinetic ions.
- Delta-f numerical scheme.
- Production size run: 5-20 wall clock hours.

# Self-consistent MHD + fast ions coupling scheme

Background plasma - fluid:

$$\rho \frac{d\mathbf{V}}{dt} = -\nabla p + (\mathbf{j} - \mathbf{j}_b) \times \mathbf{B} - n_b (\mathbf{E} - \eta \mathbf{j})$$

$$\mathbf{E} = -\mathbf{V} \times \mathbf{B} + \eta \mathbf{j}$$

$$\mathbf{B} = \mathbf{B}_0 + \nabla \times \mathbf{A}$$

$$\partial \mathbf{A} / \partial t = -\mathbf{E}$$

$$\mathbf{j} = \nabla \times \mathbf{B}$$

$$\partial p^{1/\gamma} / \partial t = -\nabla \cdot (\mathbf{V} p^{1/\gamma})$$

$$\partial \rho / \partial t = -\nabla \cdot (\mathbf{V} \rho)$$

Fast ions – delta-F scheme:

$$\frac{d\mathbf{x}}{dt} = \mathbf{v}$$

$$\frac{d\mathbf{v}}{dt} = \mathbf{E} - \eta \mathbf{j} + \mathbf{v} \times \mathbf{B}$$

$$w = \delta F / F \quad \text{- particle weight}$$

$$\frac{dw}{dt} = -(1-w) \frac{d(\ln F_0)}{dt}$$

$$F_0 = F_0(\varepsilon, \mu, p_\phi)$$

$\rho$ ,  $\mathbf{V}$  and  $p$  are thermal plasma density, velocity and pressure,  $n_b$  and  $\mathbf{j}_b$  are beam ion density and current, and  $n_b \ll n_e$  – is assumed.

# Self-consistent anisotropic equilibrium including the NBI ions

Grad-Shafranov equation for two-component plasma:

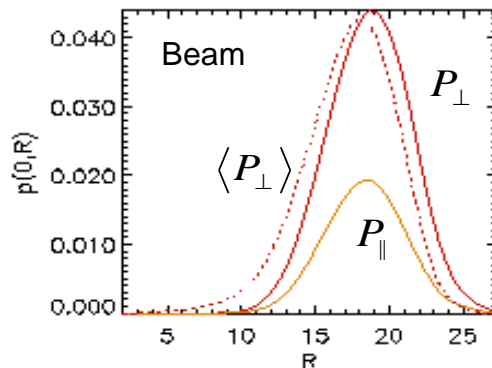
MHD plasma (thermal) and fast ions [Belova et al, Phys. Plasmas 2003].

$$\frac{\partial^2 \psi}{\partial z^2} + R \frac{\partial}{\partial R} \left( \frac{1}{R} \frac{\partial \psi}{\partial R} \right) = -R^2 p' - HH' - \underbrace{GH' + RJ_{bp}}_{\text{Beam effects}}$$

$$\mathbf{B} = \nabla \phi \times \nabla \psi + h \nabla \phi$$

$$h(R, z) = H(\psi) + G(R, z)$$

$$\mathbf{J}_{bp} = \nabla G \times \nabla \phi, \quad G - \text{poloidal stream function}$$



Modifications of equilibrium due to beam ions:

- more peaked current profile,
  - anisotropic pressure,
  - increase in Shafranov shift
- might have indirect effect on stability.

# Fast ions – delta-f scheme: $F_0 = F_0(\varepsilon, \mu, p_\phi)$

Equilibrium distribution function  $F_0 = F_1(v) F_2(\lambda) F_3(p_\phi, v)$

$$F_1(v) = \frac{1}{v^3 + v_*^3}, \text{ for } v < v_0$$

$$F_2(\lambda) = \exp(-(\lambda - \lambda_0)^2 / \Delta\lambda^2)$$

$$F_3(p_\phi, v) = \frac{(p_\phi - p_0)^\beta}{(R_0 v - \psi_0 - p_0)^\beta}, \text{ for } p_\phi > p_0$$

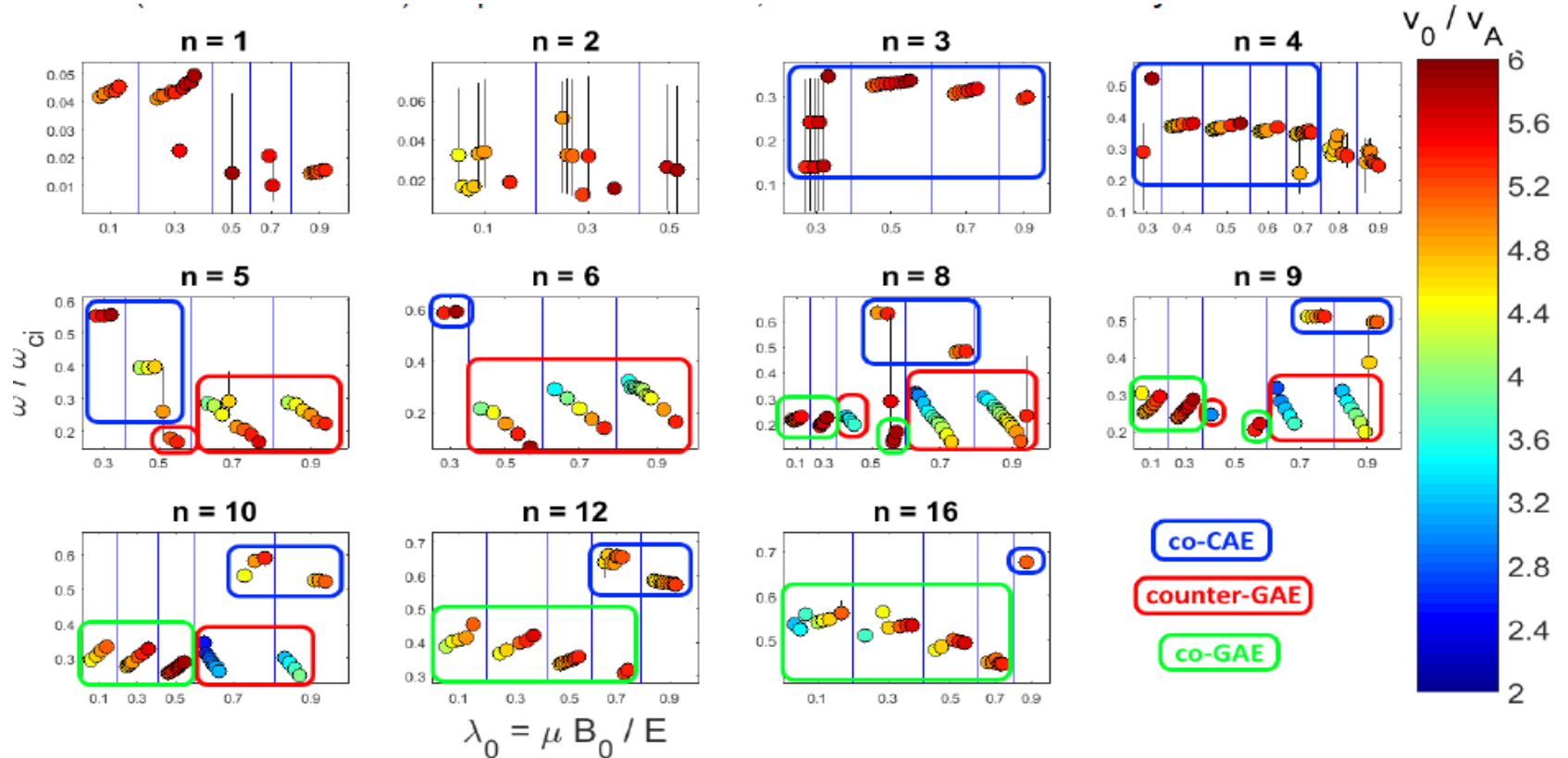
where  $v_0 = 2-5v_A$ ,  $v_* = v_0/2$ ,  $\lambda = \mu B_0 / \varepsilon$  – pitch angle parameter,  $\lambda_0 = 0.5-0.7$ , and  $\mu = \mu_0 + \mu_1$  includes first-order corrections [Littlejohn'81]:

$$\mu = \frac{(\mathbf{v}_\perp - \mathbf{v}_d)^2}{2B} - \frac{\mu_0 v_\parallel}{2B} [\hat{\mathbf{b}} \cdot \nabla \times \hat{\mathbf{b}} - 2(\hat{\mathbf{a}} \cdot \nabla \hat{\mathbf{b}}) \cdot \hat{\mathbf{c}}]$$

$\mathbf{v}_d$  is magnetic gradient and curvature drift velocity,  $\hat{\mathbf{c}} = \mathbf{v}_\perp / v_\perp$ ,  $\hat{\mathbf{a}} = \hat{\mathbf{b}} \times \hat{\mathbf{c}}$ .

Parameters are chosen to match TRANSP beam profiles.

# NSTX: Beam ion distribution parameter scan shows that many modes can be excited for $v/v_A \geq 4$ [J. Lestz, APS 2015]



## New findings:

- dependence of number of unstable CAE/GAEs on  $v_0/v_A$
- strong dependence on most unstable  $\omega$  on beam parameters for GAEs
- predicted unstable co-GAEs



# HYM simulations reproduce frequency range of unstable GAE and CAE modes observed in NSTX

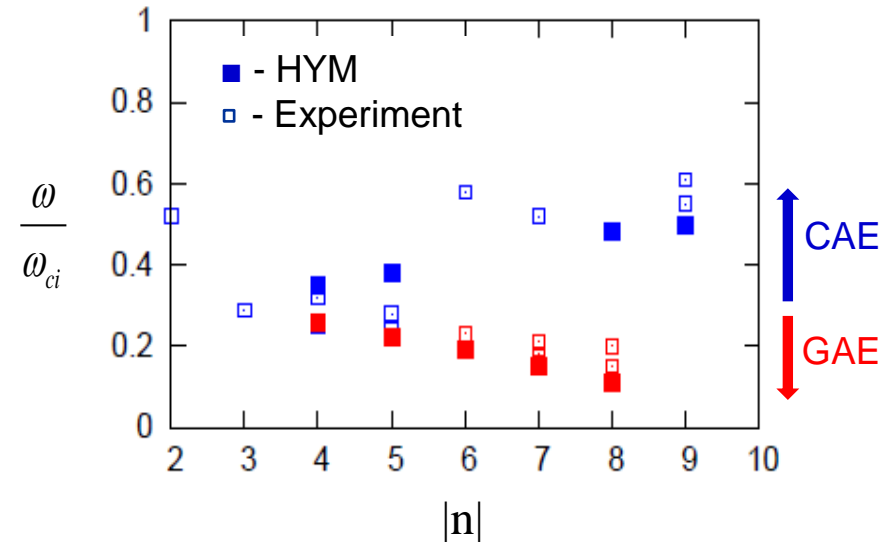
## Experimental analysis:

Detailed measurements of GAE and CAE amplitudes and mode structure for H-mode plasma in NSTX shot 141398 [N. Crocker, NF 2013].

- **CAEs**:  $f > 600$  kHz, and  $|n| \leq 5$ .
- **GAEs**:  $f < 600$  kHz, and  $|n| \sim 6-8$ .
- Co- and counter-rotating CAEs with  $f \sim 1.2-1.8$  MHz, and  $n=6-14$  also observed in the same shot [E. Fredrickson, PoP 2013].

## HYM simulations:

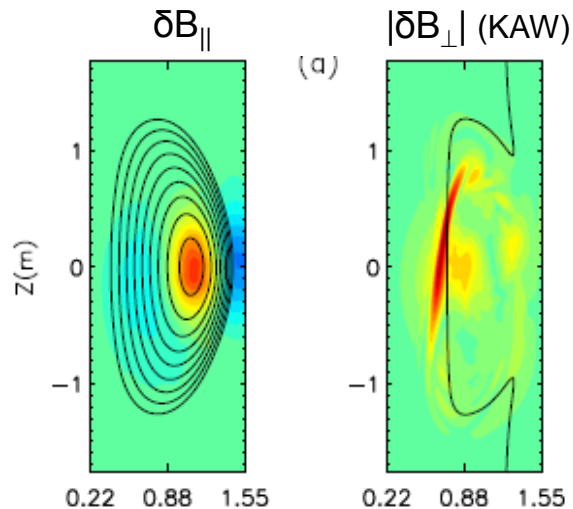
- For  $n=5-7$  most unstable are counter-rotating **GAEs**, with  $f = 380-550$  kHz.
- For  $n=4$  and  $n=8, 9$  most unstable are co-rotating **CAEs** with  $f = 870-1200$  kHz.



Frequency versus toroidal mode number for unstable GAEs (red) and CAEs (blue), from HYM simulations and experiment,  $f_{ci} = 2.5$  MHz.

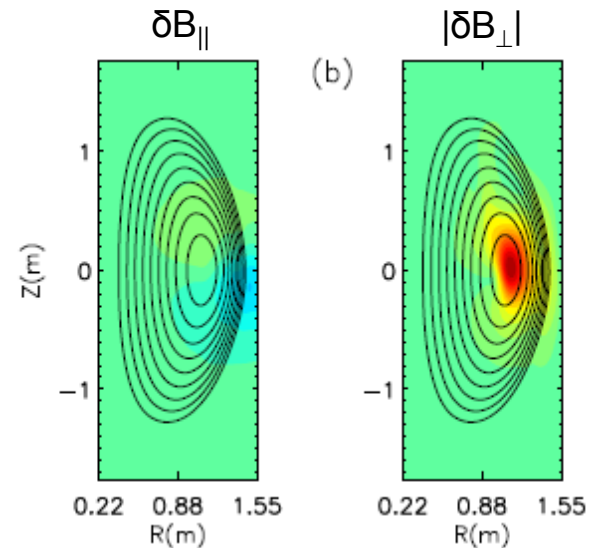
## CAE has large compressional component in the core and couples to KAW

$n=4$ , CAE



$\delta B_{\parallel}$  is significantly larger than  $\delta B_{\perp}$  at the axis.

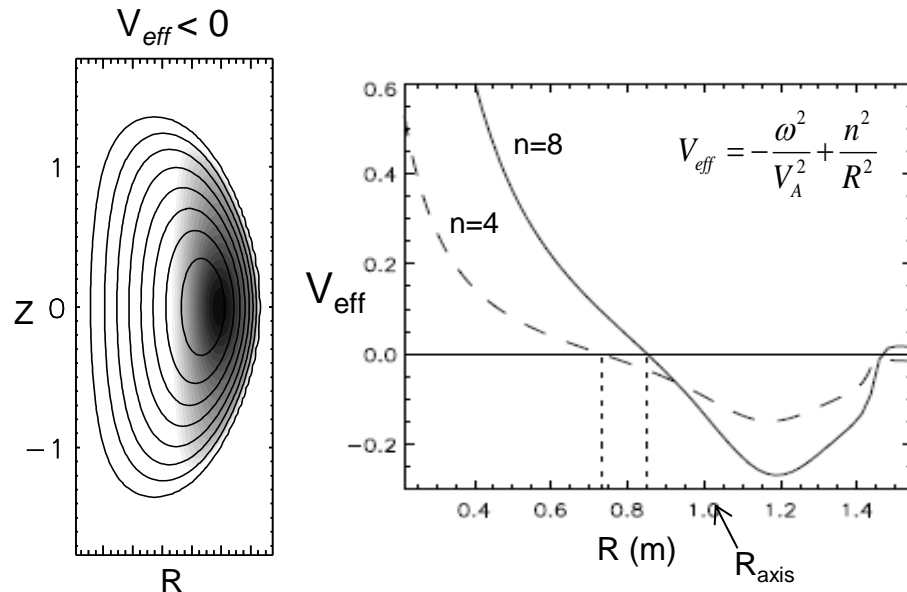
$n=6$ , GAE



$\delta B_{\parallel}$  is comparable to  $\delta B_{\perp}$  only at the edge.

- CAE/KAW coupling seen for all unstable CAEs.
- KAW has large amplitude on HFS.

# CAE/KAW coupling is universal



Contour plot and radial profile of the effective potential  $V_{eff}$  for  $n=8$  CAE mode with  $\omega=0.48\omega_{ci0}$  (solid) and  $n=4$  CAE with  $\omega=0.34\omega_{ci0}$  (dashed). Mode can exist for  $V_{eff} < 0$  with radial extent:  $0.85(0.73)\text{m} < R < 1.45\text{m}$ .

Approximate equation for CAE mode, assuming circular cross-section, and neglecting beam effects and coupling to SAW:

$$\frac{\partial^2 \delta B_{\parallel}}{\partial r^2} = V_{eff} \delta B_{\parallel}$$

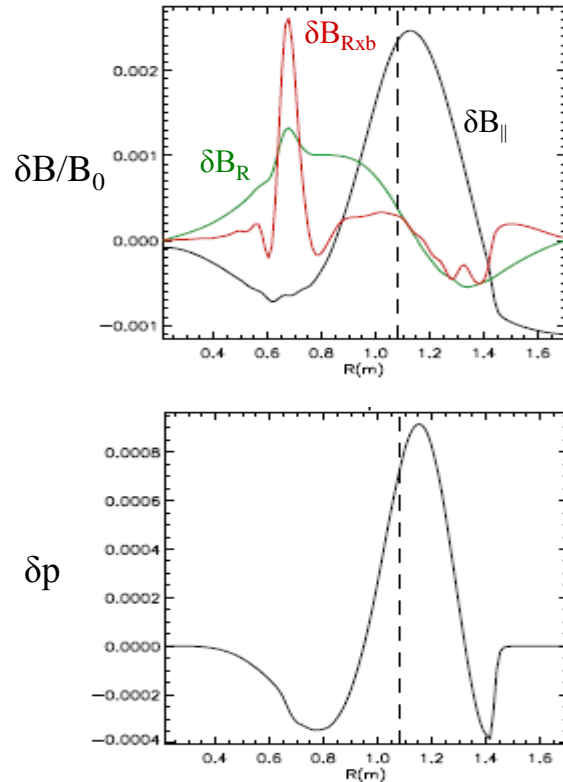
$$V_{eff} = -\frac{\omega^2}{V_A^2} + k_{\parallel}^2$$

HYM simulations show unstable  $n=8$  mode with  $\omega=0.48\omega_{ci0}$  and  $\gamma=0.004\omega_{ci0}$ .

Effective potential well for  $n=8$  mode is narrower and deeper than  $V_{eff}$  for  $n=4$  resulting in more localized CAE mode with larger frequency.

Edge of CAE well coincides with resonance location  $\rightarrow$  CAE/KAW coupling.

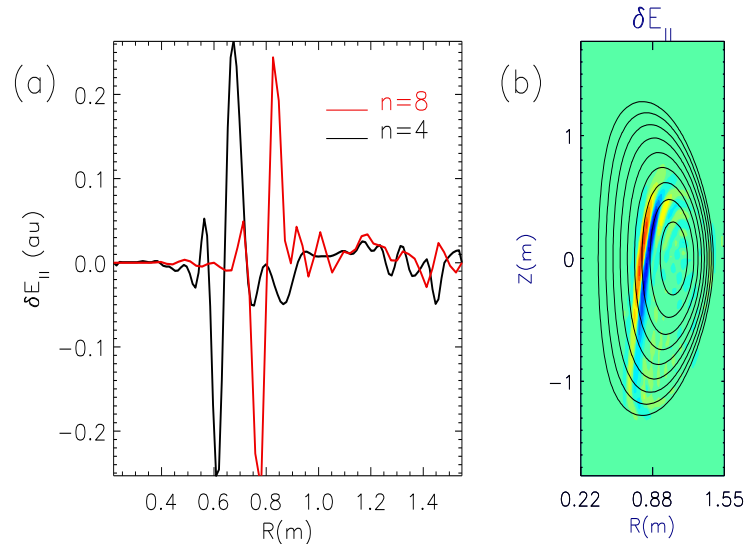
# On-axis CAE couples to off-axis KAW



Radial profiles of (a) magnetic field perturbation; and (b) normalized thermal pressure perturbation for the  $n=4$  CAE versus major radius. The CAE peaks near the magnetic axis  $R=1.07$  m.

- Radial width of KAW is determined by beam ions Larmor radius,  $k_{\perp} \sim 1/\Delta = (L\rho^2)^{-1/3}$ , where  $\rho^2 = \left(\frac{3}{4} \left[1 + \frac{\beta_b}{\beta_i}\right] + \frac{T_e}{T_i}\right) \rho_i^2$  (full kinetic model),  $\rho = \sqrt{3/4 n_b/n_e} \rho_b$  (HYM model).
- Resonant mode polarization is consistent with KAW mode, ie  $\delta B_Z \gg \delta B_R, \delta B_{||}$  and  $\delta V_Z \gg \delta V_R, \delta V_{||}$  with  $\delta V_Z \sim -\delta B_Z$ .
- $\delta B_{||}$ , perturbed pressure and plasma density show a smooth behavior across the resonance, consistent with incompressible nature of KAW.
- Resonance with KAW is located at the edge of CAE well, near the edge beam ion density profile at  $r/a \sim 0.6$ .

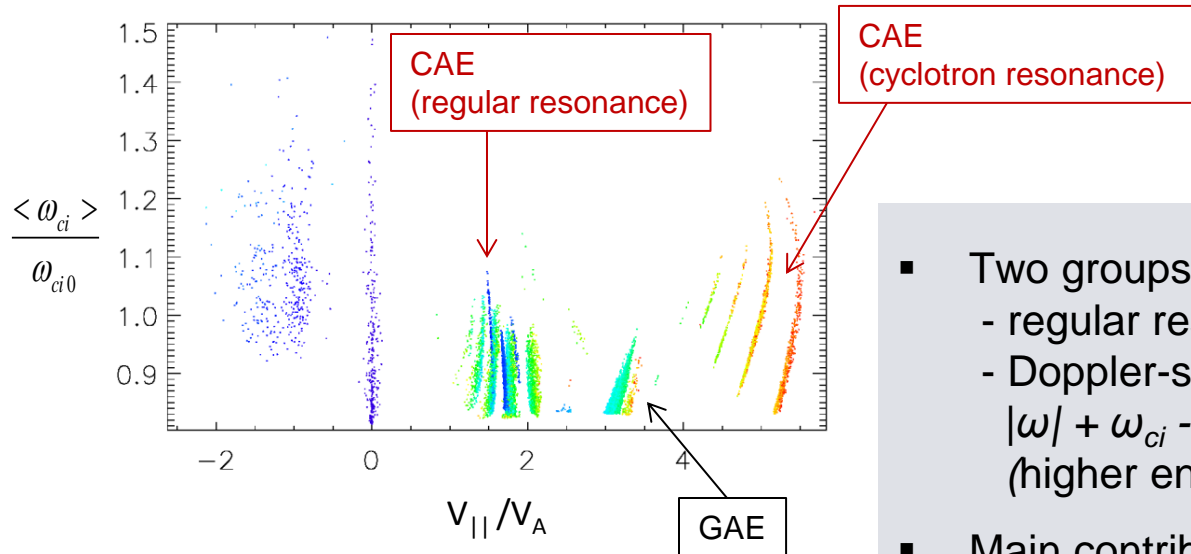
## KAW can have strong effect on electron transport due to finite $\delta E_{\parallel}$



(a) Radial profiles of  $\delta E_{\parallel}$  from CAE/KAW simulations for  $n=4$ (black) and  $n=8$  (red); (b) contour plot of  $\delta E_{\parallel}$  for the  $n=8$  CAE/KAW.

- Radial width of KAWs is relatively large on HFS in NSTX. Therefore, the KAWs will overlap radially.
- In addition to the energy channelling mechanism, several overlapping KAWs with relatively large  $\delta E_{\parallel}$  can also have a direct effect on both the electron transport and the beam ion re-distribution.
- Need to include 2-fluid effects in CAE/KAW simulations.

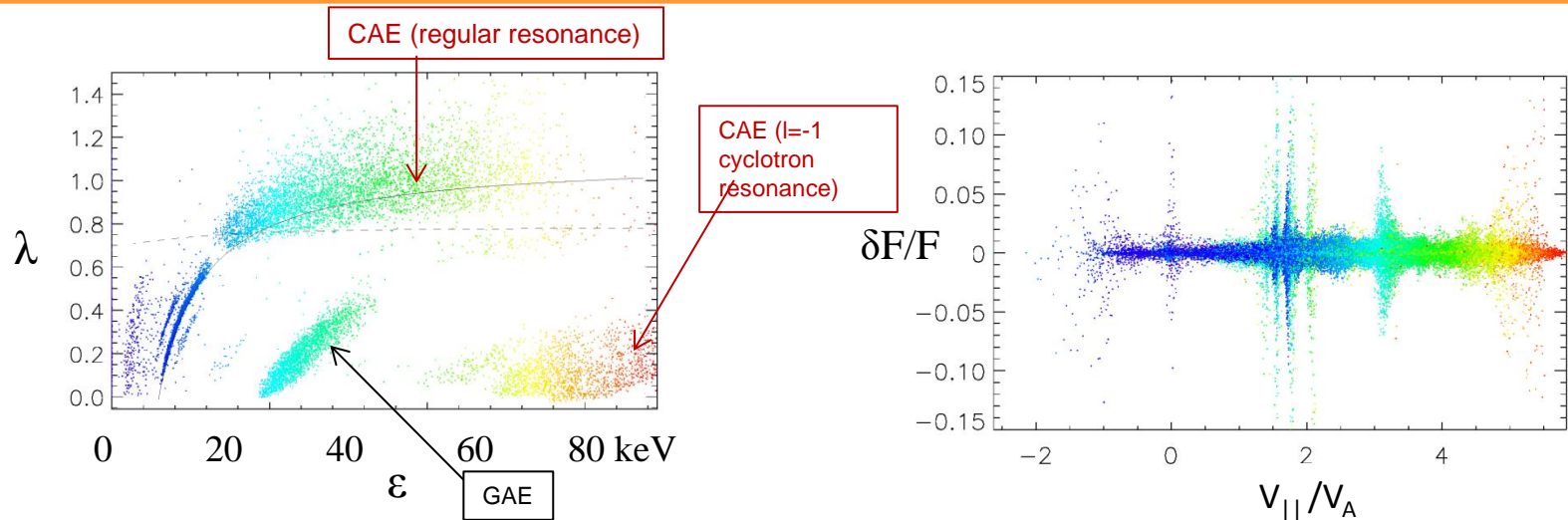
Simulations: main drive for CAE comes from resonant particles with  $v_{||} \sim \omega/k_{||}$



Orbit-averaged cyclotron frequency vs orbit-averaged parallel velocity for resonant particles. From simulations for  $n=8$  CAE ( $\omega=0.48\omega_{ci0}$ ,  $\gamma=0.004\omega_{ci0}$ ). Particle color corresponds to different energies: from  $E=0$  (purple) to  $E=90\text{keV}$  (red).

- Two groups of resonant particles:
  - regular resonance:  $\omega - k_{||}v_{||} = 0$ ,
  - Doppler-shifted cyclotron resonance:  $|\omega| + \omega_{ci} - k_{||}v_{||} = 0$  (higher energy particles).
- Main contribution comes from the beam ions with  $v_{||} \sim \omega/k_{||}$ .
- “Turning off” high-energy resonant particles does not change the growth rate  $\rightarrow$  contribution from the cyclotron resonances is negligible.

# Location of resonant particles in phase-space

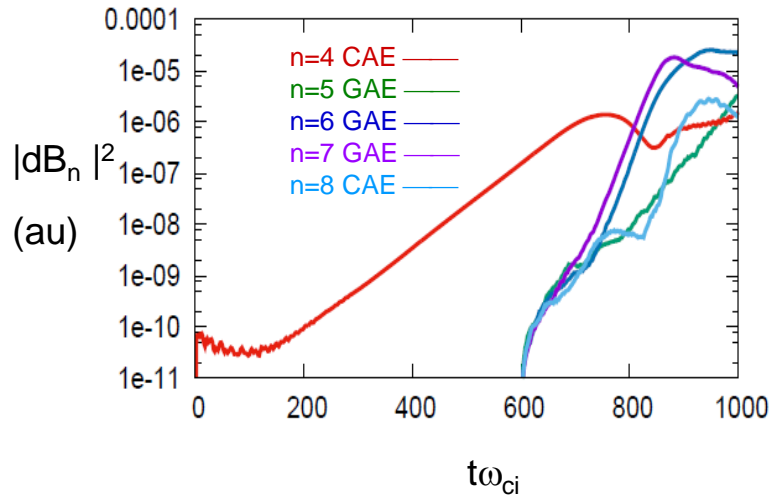


Location of resonant particles in phase space:  $\lambda = \mu B_0 / \epsilon$  vs energy. From HYM simulations for NSTX shot #141398,  $\omega = 0.48\omega_{ci0}$ ,  $\gamma = 0.004\omega_{ci0}$ . Particle color corresponds to different energies: from E=0 (purple) to E=90keV (red).

Particle weight  $w \sim \delta F/F$  vs orbit-averaged parallel velocity for all simulations particles. Particle color corresponds to different energies: from E=0 (purple) to E=90keV (red).

- Resonant velocity can be estimated as  $v_{||} \approx \omega R_0 / n = 1.7V_A$ , in good agreement with simulations.
- Distribution in  $(\lambda, \epsilon)$  space can be described approximately by a relation  $\lambda = 1 - v_{||}^2 / 2\epsilon$  for a fixed  $v_{||}$  (solid line plotted for  $v_{||} = 1.7V_A$ ).
- Instability is driven mostly by the trapped beam ions with  $D = \frac{\partial F_0}{\partial \epsilon} - \frac{\lambda}{\epsilon} \frac{\partial F_0}{\partial \lambda} > 0$ , whereas lower-energy passing ions are stabilizing (dashed line corresponds to condition  $D=0$ ).

## Nonlinear CAE simulations

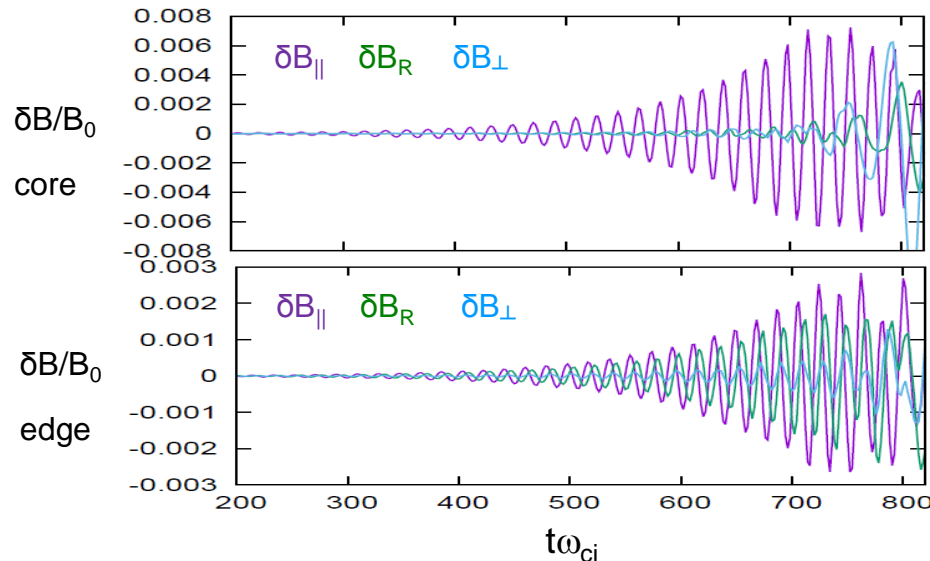


Time evolution of amplitudes of different toroidal harmonics from fully nonlinear simulations for NSTX shot 141398.

- Fully nonlinear simulations including 32 toroidal harmonics show saturation of the  $n=4$  CAE mode.
- Initial conditions for nonlinear run were obtained by running the  $n=4$  linearized simulations (from  $t=0-550$ ) to obtain a converged linear mode structure of CAE.
- Nonlinear run starts at  $t=550$ , and also shows growth of  $n=5,6,7$  GAEs and  $n=8$  CAE modes.
- $n=6$  and  $7$  GAEs have larger linear growth rates than the  $n=4$  CAE mode.



## Nonlinear simulations show CAE saturation amplitudes higher but comparable to experimentally observed

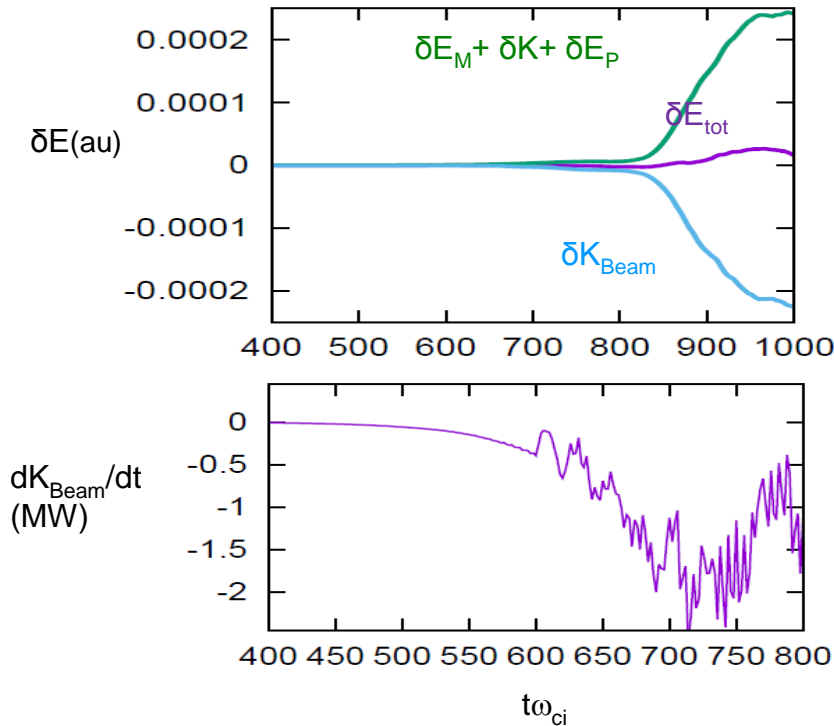


- In the core, the compressional perturbation is 3-4 times larger than the shear perturbation.
- Mixed compressional/shear polarization near the plasma edge on LFS .

Time evolution of  $\delta B_{\parallel}$  and two components of  $\delta \mathbf{B}_{\perp}$  in the core, and close to the plasma edge on LFS.

- Saturation amplitude of the  $n=4$  CAE:  $\delta B_{\parallel}/B_0 = 6.6 \times 10^{-3}$ .
- Measured plasma displacement  $|\xi| = 0.1-0.4$  mm [Crocker, 2013] corresponds to  $\delta B/B_0 = (0.9-3.4) \times 10^{-3}$  (based on HYM-calculated mode structure for  $n=4$  CAE).

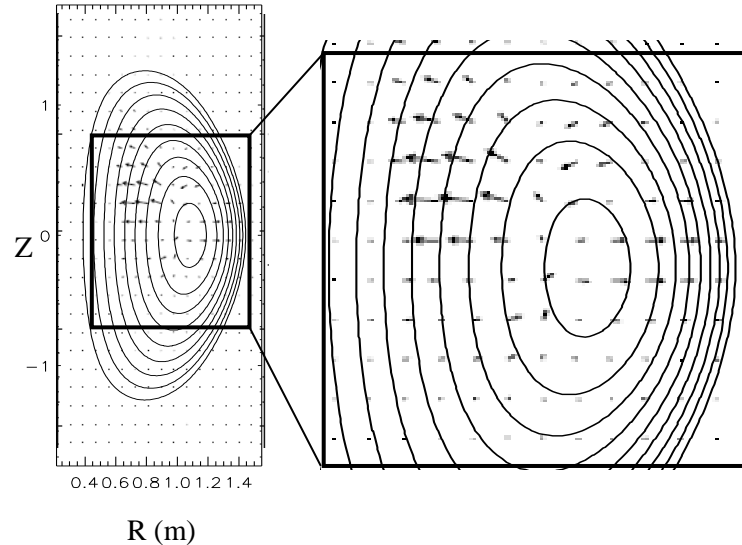
## Significant fraction of the total beam power can transferred to a single CAE of relatively large amplitude



- (a) Time evolution of the fluid energy (green), the beam ion energy (light blue), and the total energy of the system (purple);
- (b) Time evolution of rate of change of beam ion energy, calculated as  $\int (\mathbf{J}_{beam} \mathbf{E}) d^3x$ .

Rate of change of the beam ion energy is  $\sim 1.5$  MW for calculated the  $n=4$  CAE saturation amplitude  $\delta B_{||}/B_0 = 6.6 \times 10^{-3}$ .

# Energy flux is directed away from magnetic axis



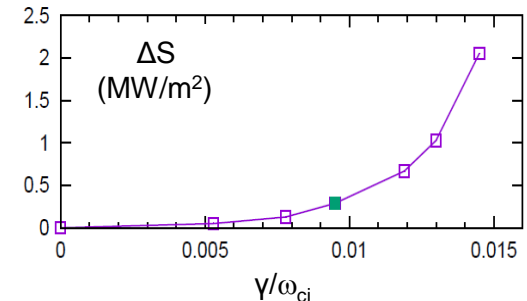
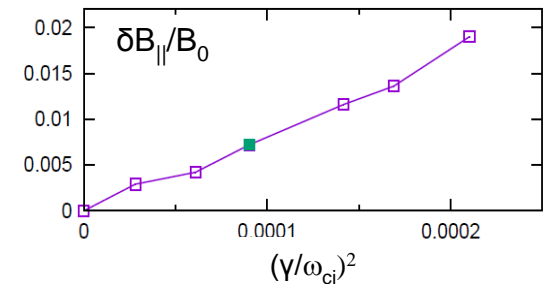
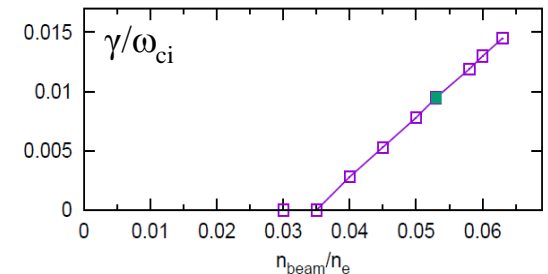
Vector plot of energy flux  
 $\mathbf{S} = \mathbf{E} \times \mathbf{B} / 4\pi + p\mathbf{V} / (\gamma - 1)$ .

Energy flux is directed away from magnetic axis, towards both high- and low-field side. LFS resonance is more diffuse compared to HFS. From the self-consistent nonlinear simulations of the  $n=4$  CAE mode near saturation.

Change of energy flux across resonant layer at  $R \sim 0.7\text{m}$  is  $S_R \sim 0.8 \times 10^5 \text{ W/m}^2$ , which corresponds to power absorption at the high-field-side resonance of  $P \sim 0.2 \text{ MW}$  for  $\delta B_{||} / B_0 \sim 3 \times 10^{-3}$ .

# CAE-to-KAW energy channeling shows strong scaling with the beam power

- From density threshold – damping rate due to CAE/KAW coupling is large  $\gamma_{\text{damp}} = 0.66 \gamma_{\text{dr}}$ .
- Threshold value of the beam power needed for the excitation of the  $n=4$  CAE can be estimated as  $P \sim 4\text{MW}$ .
- Instability saturates nonlinearly due to particle trapping, and  $\delta B_{\parallel}/B_0 \sim (\gamma/\omega_{\text{ci}})^2$ .
- Absorption rate shows a very strong scaling with growth rate:  $\Delta S \sim (\gamma/\omega_{\text{ci}})^5$ , implying that the energy loss at the resonance scales as a fifth power of the beam ion density (beam power).



## CAE/KAW coupling can provide an efficient energy channeling mechanism, and can have direct effect on the $T_e$ profiles.

- Simulations show unstable CAE modes for toroidal mode numbers  $n=4-9$  in H-mode NSTX discharges.
- Unstable CAE modes couple with KAW on the HFS. Resonance with KAW is located at the edge of CAE well, and just inside beam ion density profile. Radial width of KAW is determined by beam ion Larmor radius.
- A significant fraction of NBI energy can be transferred to several unstable CAEs: up to  $P \sim 0.4 \text{ MW}$  for one mode with  $\delta B/B_0 \sim 3 \times 10^{-3}$ .
- Energy flux is shown to be directed away from the magnetic axis (CAE) toward the resonance location (KAW); power absorption at the high-field-side resonance of  $P \sim 0.2 \text{ MW}$  for  $\delta B_{\parallel}/B_0 \sim 3 \times 10^{-3}$ .
- Strong CAE/KAW coupling follows from dispersion relation, therefore, this mechanism applies to any device with unstable CAEs.
- Absorption rate shows a very strong scaling with growth rate:  $\Delta S \sim (\gamma/\omega_{ci})^5$ , implying that the energy loss at the resonance scales as a fifth power of the beam power.

# Future Plans

---

## Code development

- Improve the fast ion distribution function model.
- Include thermal ions kinetic effects (Hall, FLR) and bulk plasma rotation.

## Physics

- Understanding conditions for preferential excitation of GAEs and CAEs.
- Comparison of the relative importance of the energy channeling vs anomalous electron transport mechanisms.
- Comparison with experimental results including mode structure, saturation amplitudes and etc for several shots.
- Continue NSTX-U simulations – GAEs stabilization.